Molecular Cancer Therapeutics

Modulating Therapeutic Activity and Toxicity of Pyrrolobenzodiazepine Antibody–Drug Conjugates with Self-Immolative Disulfide Linkers

Thomas H. Pillow[1], Melissa Schutten[1], Shang-Fan Yu[1], Rachana Ohri[1], Jack Sadowsky[1], Kirsten Achilles Poon[1], Willy Solis[1], Fiona Zhong[1], Geoffrey Del Rosario[1], Mary Ann T. Go[1], Jeffrey Lau[1], Sharon Yee[1], Jintang He[1], Luna Liu[1], Carl Ng[1], Keyang Xu[1], Douglas D. Leipold[1], Amrita V. Kamath[1], Donglu Zhang[1], Luke Masterson[2], Stephen J. Gregson[2], Philip W. Howard[2], Fan Fang[3], Jinhua Chen[3], Janet Gunzner-Toste[1], Katherine K. Kozak[1], Susan Spencer[1], Paul Polakis[1], Andrew G. Polson[1], John A. Flygare[1], and Jagath R. Junutula[1]

Abstract

A novel disulfide linker was designed to enable a direct connection between cytotoxic pyrrolobenzodiazepine (PBD) drugs and the cysteine on a targeting antibody for use in antibody–drug conjugates (ADCs). ADCs composed of a cysteine-engineered antibody were armed with a PBD using a self-immolative disulfide linker. Both the chemical linker and the antibody site were optimized for this new bioconjugation strategy to provide a highly stable and efficacious ADC. This novel disulfide ADC was compared with a conjugate containing the same PBD drug, but attached to the antibody via a peptide linker. Both ADCs had similar efficacy in mice bearing human tumor xenografts. Safety studies in rats revealed that the disulfide-linked ADC had a higher MTD than the peptide-linked ADC. Overall, these data suggest that the novel self-immolative disulfide linker represents a valuable way to construct ADCs with equivalent efficacy and improved safety. *Mol Cancer Ther; 16(5); 871–8. ©2017 AACR.*

Introduction

Antibody–drug conjugates (ADCs) have proven to be an effective method of selectively delivering a small cytotoxic payload to a targeted cell. There are over 55 ADCs currently in human clinical testing and the approval of ADCETRIS (brentuximab vendotin) and KADCYLA (ado-trastuzumab emtansine) has spurred interest in expanding the utility and scope of these powerful agents (1–3). The antibody, linker, and payload of an ADC all play a large and synergistic role in modulating the efficacy and toxicity of the conjugate. A variety of different cytotoxic payloads have been effectively attached to an antibody to produce potent conjugates. These include microtubule-disrupting drugs such as maytansines (4) and auristatins (5), as well as DNA damaging agents such as duocarmycins (6), calicheamicins (7), pyrrolobenzodiazepines (PBDs) (8), and indolinobenzodiazepines (IGNs) (9). Although the above-referenced ADCs are quite efficacious in preclinical studies, many have found limited use clinically due to a low therapeutic index, supporting a need to discover ADCs with an improved efficacy and safety profile.

Although the linker connecting these cytotoxic drugs to the antibody plays a critical role in the stability of the ADC and release of the payload (10), few studies have looked systematically at the impact of linker on efficacy and safety. Most work has focused on site-specific and stable conjugation chemistry rather than changing the mechanism by which the linker is cleaved and payload is released (11–13). Although there exist several ADC linker types (hydrazone, disulfide, peptide, glucuronide, noncleavable), each with distinct mechanisms of release [acid, glutathione (GSH), protease, glucuronidase, antibody catabolism], these linkers typically release unique metabolites, thereby obscuring the impact of the linker release mechanism itself on efficacy and toxicity (14–17). Although the β-glucuronide and peptide linkers were designed to release the same metabolite in two reported ADCs, and efficacy differences were observed, pharmacokinetic data were not provided and the only data around tolerability reported was body weight loss in mice (18).

The general dogma is that ADCs with non-cleavable linkers are often safer but less broadly efficacious. In support of this, a noncleavable linker gave an improved preclinical safety profile over a cleavable disulfide linker with maytansinoid ADCs (19). Yet in lymphoma models, the same ADC with a noncleavable linker was inferior in therapeutic activity to the ADC with a cleavable disulfide (20). The safety improvement is likely an effect of the increased stability of the noncleavable linker, requiring

[1]Genentech, Inc., South San Francisco, California. [2]Spirogen Ltd., QMB Innovation Centre, London, United Kingdom. [3]WuXi AppTec Co., Ltd., Shanghai, P.R. China.

Note: Supplementary data for this article are available at Molecular Cancer Therapeutics Online (http://mct.aacrjournals.org/).

Current address for K. Poon: Denali Therapeutics, South San Francisco, California; current address for W. Solis, Bristol Myers Squibb, Princeton, New Jersey; current address for J.R. Junutula, Cellerant Therapeutics, San Carlos, California.

Corresponding Author: Thomas H. Pillow, Genentech, Inc., South San Francisco, CA 94030. Phone: 650-225-1652; Fax: 650-467-5155; E-mail: thomashp@gene.com

doi: 10.1158/1535-7163.MCT-16-0641

antibody catabolism combined with release of an amino acid-containing non-diffusible catabolite that does not enter neighboring cells devoid of target. This is simultaneously the Achilles heel of the noncleavable linker, as this catabolite does not permit a bystander effect, limiting efficacy in models with poor penetration or antigen heterogeneity.

To potentially improve safety while maintaining efficacy, we set out to design a stably-linked ADC that would require antibody catabolism while enabling transformation of the initially-formed non-diffusible catabolite to a cell-permeable active species. To accomplish this, we used a novel disulfide linker that is afforded circulation stability through connection directly to the cysteine of an engineered antibody at a specific site (21). This stability is reversed upon degradation of the antibody, allowing facile reduction of the now-reactive disulfide by reducing agents such as GSH in the cytosol.

Although disulfide linkers have been used in the construction of ADCs for more than 30 years, they have almost exclusively been limited to the connection of thiol-containing drugs to the lysines of antibodies through heterobifunctional linkers (4). There are several limitations to these disulfide-linked conjugates. By relying on a lysine conjugation, the resulting ADCs are heterogeneous mixtures with complicated analytics and a potentially reduced therapeutic index (22, 23). Furthermore, the stability and release are paradoxically coupled in disulfide ADCs; strategies to improve circulation stability simultaneously decrease the ADC's ability to release the free drug in the target cell. Finally, although disulfide-containing ADCs have been applied to thiol-containing drugs, they are not readily applicable to the amine-containing drugs found in the vast majority of ADCs.

We addressed both the heterogeneity and the coupling of stability and release by a novel bioconjugation strategy of directly connecting the thiol of a maytansine drug to the thiol of a cysteine-engineered antibody (21). We envisioned the incorporation of a self-immolative spacer to connect the disulfide linker to an amine-containing drug, such as the nitrogen of PBD dimers (24). By varying that location through cysteine mutants, we hoped to find a site that was uniquely stable for PBD disulfide conjugates. This stability, afforded by a protective site, would then be unsheathed following release of the cysteine disulfide drug adduct upon antibody catabolism in the cell. Exposure of this disulfide to the reducing conditions of the cytosol would afford good cleavage and following immolation, release of free drug. With linker cleavage relying on antibody degradation, we hoped to maintain efficacy while decreasing toxicity. To assess, we aimed to compare the efficacy and toxicity of this novel disulfide-linked PBD ADC to that of a peptide-linked version.

Materials and Methods

Preparation of ADCs

In general, conjugates were prepared by reacting the two engineered Cys residues on antibodies with activated disulfide analogs of the PBD linker-drugs. Antibodies were produced in CHO cells and purified using standard methods. In these antibodies, the engineered Cys residues are present as mixed disulfides with cysteine or glutathione, which must be removed ("deblocked") to enable conjugation to the engineered Cys sulfhydryl groups. To accomplish this, the antibodies were partially reduced with DTT, purified, reoxidized with dehydroascorbic acid (DHAA), and purified again into a succinate buffer (10 mmol/L succinate, pH 5.0, 150 mmol/L NaCl, 2 mmol/L EDTA) to give the deblocked cysteine-engineered antibody. The pH of the deblocked antibody was adjusted with 1M Tris, pH 8.5 (75 mmol/L final Tris concentration). To the pH-adjusted antibody solution was added three equivalents of nitropyridyl disulfide PBD linker-drugs (10 mmol/L stock in dimethylformamide or DMF) suitably diluted to give 10% DMF in the final reaction solution. The conjugation reactions were allowed to proceed at room temperature until completion as indicated by LC/MS analysis of the reaction mixture (3–4 hours). Reaction mixtures were diluted five-fold into 20 mmol/L histidine-acetate, pH 5.5 buffer and loaded onto S maxi strong-cation exchange columns (Pierce), washed several times with histidine-acetate, and eluted in 20 mmol/L histidine-acetate, pH 5.5, 300 mmol/L NaCl. Conjugates were formulated into 20 mmol/L histidine-acetate, pH 5.5, 240 mmol/L sucrose by dialysis. Conjugates were analyzed for drug-to-antibody ratio (DAR) by partial digestion with LysC and reverse-phase LC/MS (PLRP-S column, Agilent TOF instrument), for aggregation by analytical SEC (Shodex column, Agilent HPLC instrument) and for endotoxin by LAL assay (Charles River instrument). All conjugates had DAR values of 1.8 to 2.0, were >98.5% monomeric and had endotoxin levels <0.1 EU/mg.

In vivo efficacy

All animal studies were carried out in compliance with National Institutes of Health guidelines for the care and use of laboratory animals and were approved by the Institutional Animal Care and Use Committee at Genentech, Inc. The efficacy of the anti-HER2 ADCs was investigated in a mouse allograft model of MMTV-HER2 Founder #5 (murine mammary tumor). The MMTV-HER2 Founder #5 (Fo5) model (developed at Genentech) is a transgenic mouse model in which the human HER2 gene, under transcriptional regulation of the murine mammary tumor virus promoter (MMTV-HER2), is overexpressed in mammary epithelium. The overexpression causes spontaneous development of mammary tumors that overexpress the human HER2 receptor. The mammary tumor from one of the founder animals (founder #5, Fo5) has been propagated in FVB mice (Charles River Laboratories) by serial transplantation of tumor fragments. For efficacy studies, the Fo5 transgenic mammary tumor was surgically transplanted into the thoracic (#2/3) mammary fat pads of female nu/nu mice (Charles River Laboratories, Hollister, CA) as tumor fragments of approximately 2 mm × 2 mm in size. The efficacy of anti-CD22 antibody drug conjugates was evaluated in a mouse xenograft model of WSU-DLCL2 human non-Hodgkin lymphoma. The WSU-DLCL2 cell line was obtained from DSMZ (German Collection of Microorganisms and Cell Cultures) in 2006. This cell line was authenticated by short tandem repeat (STR) profiling using the Promega PowerPlex 16 System and compared with external STR profiles of cell lines to determine cell line ancestry and confirmed to be mycoplasma negative. To set up the model, tumor cells (20 million cells in 0.2 mL Hank's balanced salt solution, Hyclone) were inoculated subcutaneously into the flanks of female CB17 SCID mice (Charles Rivers Laboratories). When mean tumor size reached the desired volume, the mice were divided into groups of $n = 5$, each with similar mean tumor size, and received a single intravenous injection of antibody drug conjugates through the tail vein. The treatment information was

not blinded during tumor measurement. Tumors were measured in two dimensions (length and width) using calipers and the tumor volume calculated using the formula: Tumor size (mm^3) = 0.5 × (length × width × width). The results were plotted as mean tumor volume ± SEM of each group over time. Blood samples were collected at 1, 4 and 7 days post-dose via retro-orbital bleeds and used to derive plasma for total antibody concentrations by ELISA and stability analysis by affinity capture LC/MS.

In vivo stability

To determine the *in vivo* stability of ADCs, affinity capture LC/MS was performed as described previously (25). Briefly, human HER2 and CD22 extracellular domain (ECD) was biotinylated and immobilized onto streptavidin-coated paramagnetic beads (Invitrogen) in a 96-well plate, and then the ECD-bead system was used to capture anti-CD22 disulfide conjugates by incubating with approximately 40 µL of mouse plasma samples for 2 h at room temperature. The captured ADCs were then washed with HBS-EP buffer [10 mmol/L Hepes (pH 7.4), 150 mmol/L NaCl, 3.4 mmol/L ethylenediaminetetraacetic acid (EDTA), 0.005% Surfactant P20; GE Healthcare] and deglycosylated using N-glycanase (Prozyme) at 37°C overnight. After extensive washing of the beads with HBS-EP, water, and 10% acetonitrile, the ADC analytes were eluted using 30% acetonitrile in water with 1% formic acid. A KingFisher 96 magnetic particle processor (Thermo Electron) was used to mix, wash, gather, and transfer the paramagnetic beads in the above steps. A volume of 10 µL of the eluents was analyzed by LC/MS using a TripleTOF 5600 mass spectrometer (AB Sciex). Chromatographic separation of ADCs was performed on a nanoACQUITY UPLC system (Waters Corporation) equipped with a PS-DVB monolithic column (500 µm i.d. × 5 cm; Thermo Scientific). Raw data were deconvoluted using Analyst TF 1.6 software, and the average DAR was calculated based on the peak areas of different DAR species (DAR0–DAR2).

Rat toxicity studies

To investigate the toxicity and tolerability of disulfide-linked versus peptide-linked PBD ADCs, single-dose studies were conducted in Sprague–Dawley rats. Rats were dosed intravenously on Day 1 with vehicle alone, 2.5, 5, or 7.5 mg/kg anti-HER2-(Tmab)-SG3203 (peptide-linked) or 5 or 10 mg/kg anti-HER2-(7C2)-SG3451 (disulfide-linked; $n = 5$ male animals/group). Assessment of toxicity was based on mortality, clinical signs, and clinical and anatomic pathology. Blood collections for hematology and clinical chemistry were collected in all animals on days 5 and 12. Additional blood collections for toxicokinetic (TK) analysis were taken on days 5 and 12 and were assessed by ELISA to determine limited total antibody concentrations. Necropsies were performed on day 12 and tissues were routinely processed for histologic examinations.

Results

Structure of PBD ADCs

We designed and synthesized peptide-linked (SG3203) and disulfide-linked ADCs (SG3231, SG3451) that release the PBD dimer SG2057 (refs. 26, 27; Fig. 1; Supplementary Methods and Materials). The putative mechanism of linker release for the peptide linker (SG3203) is cleavage by proteases such as cysteine-cathepsins in the lysosome followed by an immolative elimination to generate the PBD dimer SG2057 (Fig. 1A). For the disulfide linkers (SG3231, SG3451), the antibody is likely first degraded in the lysosome to generate a cysteine-disulfide catabolite followed by disulfide reduction in the cytosol by cellular reductants such as GSH (Fig. 1B). The free thiol is now poised to undergo a three-membered ring episulfide forming-cyclization reaction to release SG2057 (21, 28–30), the exact same free drug released by the peptide linker.

Optimization of disulfide-linked PBD ADCs through antibody site and linker substitution

We selected the unhindered disulfide linker (SG3231) for the preliminary evaluation of PBD ADCs. This linker-drug was connected to a cysteine-engineered antibody at either V205C or K149C of the light chain (LC). *In vivo* stability was measured in mice (Fig. 2A). The disulfide connected to V205C was not

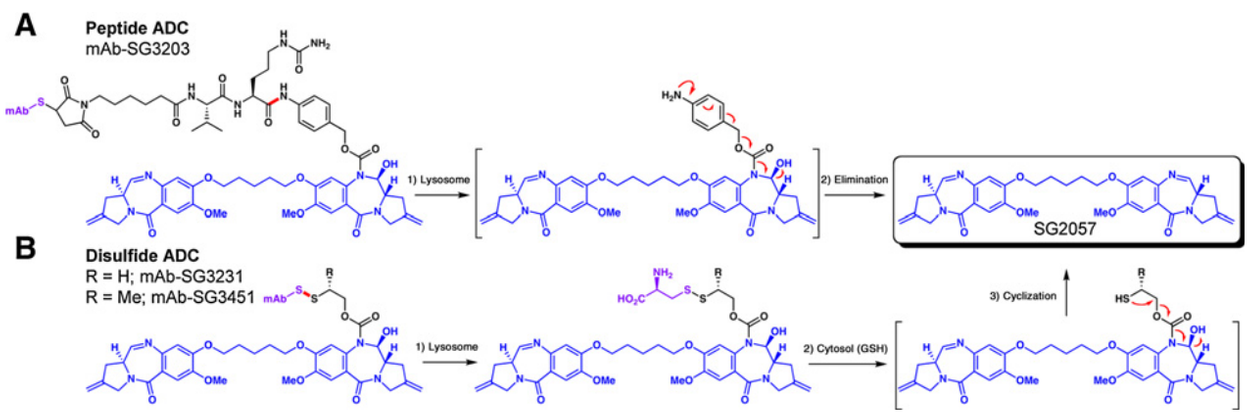

Figure 1.
Peptide- and disulfide-linked PBD ADCs. **A,** The ADC with a peptide linker (SG3203) is degraded in the lysosome to generate a reactive intermediate that undergoes immolative elimination to release free drug SG2057. **B,** The ADCs with disulfide linkers (SG3231, SG3451) are degraded in the lysosome to a putative cysteine catabolite that undergoes disulfide reduction in the cytosol by cellular reductants such as GSH, followed by an episulfide cyclization to release free drug SG2057.

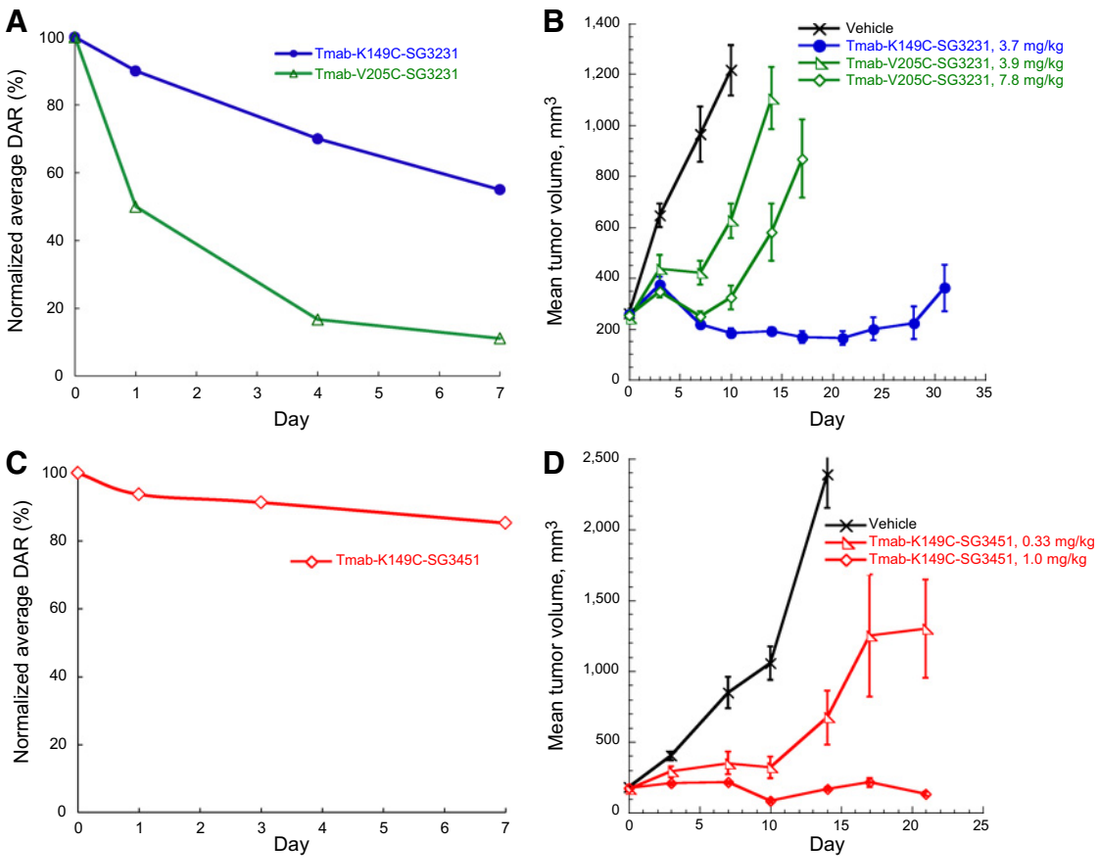

Figure 2.

In vivo stability and efficacy of disulfide PBD ADCs. **A,** *In vivo* stability of unhindered disulfide PBD (SG3231) ADCs in mice, with the disulfide linker directly connected to a cysteine mutant at different sites of the antibody (LC-V205C or LC-K149C). The nu/nu mice were dosed intravenously with ∼ 4 mg/kg (98 μg/m^2 drug dose) of Tmab-SG3231 (V205C or K149C). At the indicated time points, blood was drawn for determination of the average DAR normalized to day 0 using an affinity-capture LC/MS method. **B,** *In vivo* efficacy of unhindered disulfide PBD (SG3231) ADCs at different sites in a HER2+ Fo5 mammary tumor transplant mouse model. Fragments (approximately 2 × 2 mm) of MMTV-HER2 Fo5 transgenic mammary tumors were surgically transplanted into the number 2/3 mammary fat pads of nu/nu mice. The tumor-bearing animals were randomized to a mean tumor volume range of ∼250 mm^3 and administered a single intravenous dose (day 0) of vehicle or Tmab-SG3231 at ∼4 or ∼8 mg/kg (98 or 197 μg/m^2 drug dose). Mean tumor volumes (±SEM) are plotted over time (days post dose). **C,** *In vivo* stability of a methyl disulfide PBD (SG3451) ADC in mice with the disulfide linker directly connected to the cysteine mutant K149C. The nu/nu mice were dosed intravenously with ∼1 mg/kg (22 μg/m^2 drug dose) of Tmab-SG3451 (K149C). **D,** *In vivo* efficacy of a methyl disulfide PBD (SG3451) ADC in a HER2+ Fo5 mammary tumor transplant mouse model. The tumor-bearing animals were randomized to a mean tumor volume of ∼175 mm^3 and administered a single intravenous dose (day 0) of vehicle or Tmab-SG3451 (K149C) at 0.33 or 1 mg/kg (7 or 22 μg/m^2 drug dose).

stable, with approximately half of the drug deconjugating by 1 day. In contrast, the K149C site stabilized this unhindered disulfide, enabling the conjugate to retain more than half of the drug for 7 days. The antitumor activity of these two conjugates was then determined in a HER2+ Fo5 tumor transplant model (Fig. 2B). Consistent with the *in vivo* stability results, the more stable conjugate at K149C was also more efficacious, giving tumor stasis at a dose of 3.7 mg/kg whereas the unstable conjugate at V205C did not achieve this level of activity even at twice the dose (7.8 mg/kg). To further increase disulfide stability, we incorporated an additional methyl group in the linker adjacent to the disulfide, resulting in methyl disulfide PBD (SG3451; Fig. 1B). This additional methyl group resulted in a very stable connection to the K149C site (Fig. 2C) with approximately 85% of the drug remaining attached to the antibody after 7 days. The additional methyl also increased the rate of free PBD (SG2057) release (Supplementary Fig. S1). This increased stability and release of drug resulted in a highly efficacious conjugate (SG3451) with tumor stasis at a dose of 1 mg/kg and significant tumor growth inhibition observed even at 0.33 mg/kg (Fig. 2D).

Efficacy of peptide and optimized disulfide PBD ADCs

We then compared the efficacy of an ADC with a disulfide linker (SG3451) to that of a peptide linker (SG3203). Because of differences in stabilities between maleimide and disulfide conjugation chemistries, different antibody sites were selected for the respective ADCs. We picked site HC-A118C for the maleimide peptide-linked PBD ADC (SG3203) to provide a stability profile similar to that of the disulfide-linked PBD ADC (SG3451) on site LC-K149C (Supplementary Fig. S2). We then evaluated the two ADCs for efficacy in mice in WSU-DLCL2, a

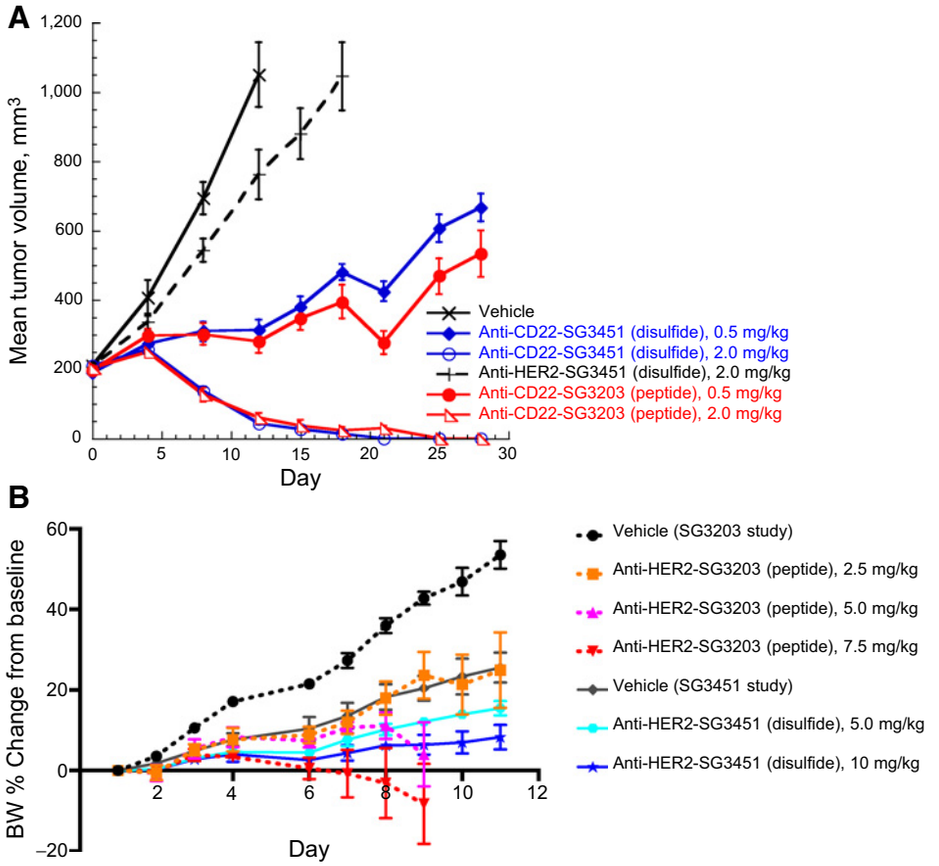

Figure 3.
Efficacy and toxicity of peptide and disulfide PBD ADCs. **A,** *In vivo* efficacy of anti-CD22-SG3451 (disulfide) and anti-CD22-SG3203 (peptide) in mice bearing WSU-DLCL2 human non-Hodgkin lymphoma xenografts. SCID mice were subcutaneously implanted with ~20 million tumor cells and administered a single intravenous dose (day 0) of vehicle, anti-HER2 (negative control), or anti-CD22 conjugates at 0.5 and 2 mg/kg when average tumor volume reached ~200 mm^3. Mean tumor volumes (±SEM) are plotted over time (days post dose). **B,** Effect of anti-HER2-SG3451 and anti-HER2-SG3203 ADCs on body weight in rats. A single intravenous dose of anti-HER2-SG3203 (dotted lines) resulted in body weight loss at ≥ 5 mg/kg and the corresponding animals were euthanized early due to adverse clinical observation, body weight loss and moribundity. Single intravenous dose of anti-HER2-SG3451 (solid lines) resulted in decreases in body weight gained compared to its concurrent control. Mean body weights (% change from baseline) ±SD are plotted over time (days post dose).

human non-Hodgkin lymphoma tumor xenograft relatively resistant to MMAE ADCs (31). Both PBD conjugates were highly efficacious, resulting in complete tumor regression at 2 mg/kg with no measurable tumor after 36 days, whereas significant tumor growth inhibition was observed for both conjugates at 0.5 mg/kg (Fig. 3A). The peptide and disulfide conjugates had similar activity at several doses and this finding was observed in additional studies in a distinct xenograft model (Supplementary Fig. S3). The exposure of the ADCs with the disulfide linker (SG3451) and the peptide linker (SG3203) were also explored in this efficacy study. Following the single IV dose of anti-CD22-SG3203 and anti-CD22-SG3451 at 2.0 mg/kg, the two ADCs demonstrated overall a similar total antibody exposure (Supplementary Fig. S4). Total antibody area under the curve from days 1 to 7 (AUC_{1-7}) also confirmed similar total antibody exposure, at 64.5 and 82.9 day•μg/mL, respectively.

Toxicity of peptide and optimized disulfide PBD ADCs

In general, a single dose of anti-HER2-SG3203 or anti-HER2-SG3451 in rats ($n = 5$/group) was well-tolerated at 2.5 mg/kg and up to 10 mg/kg, respectively. SG3203 was not tolerated at the higher doses of 5 and 7.5 mg/kg with clinical observations including perinasal, paw, and head swelling, as well as body weight loss (Fig. 3B). These clinical observations correlated microscopically with subcutaneous edema, fibrin deposition, and necrosis. Because of the clinical observations, body weight loss and general declining condition, animals were euthanized on day 9 for humane reasons.

The main toxicity observed for peptide-linked anti-HER2-SG3203 was bone marrow hypocellularity that correlated with hematologic findings of pancytopenia (decreases in red cell mass, reticulocytes, white cell counts, and platelets). Pancytopenia persisted from day 5 through the end of study. Clinical chemistry findings included increased liver enzymes, including gamma-glutamyl transpeptidase (GGT), at 2.5 mg/kg with no histopathology correlates. Additional changes in histopathology included decreased lymphoid cellularity of thymus, spleen, and lymph nodes; increased alveolar macrophages in the lung; and epithelial/crypt degeneration in the small and large intestines.

In contrast, disulfide-linked anti-HER2-SG3451 was tolerated up to 10 mg/kg with decreases in mean body weight gained compared to the concurrent vehicle control groups (Fig. 3B). One rat at 10 mg/kg developed perinasal swelling at day 12, correlating microscopically to subcutaneous edema and epidermal crusting. Similar to but less severe than anti-HER2-SG3203, the main toxicity observed with anti-HER2-SG3451 was bone marrow hypocellularity (Supplementary Fig. S5). There were no changes in clinical chemistry parameters. Additional anatomic pathology changes included decreased lymphoid cellularity in the thymus and spleen and increased alveolar macrophages in the lung.

Decreased aggregation associated with disulfide PBD ADCs

To evaluate aggregation, anti-HER2-SG3203 (peptide) and anti-HER2-SG3451 (disulfide) ADCs were prepared at a drug loading or DAR of both 2 and 4. Aggregation levels were measured both before and after purification. Aggregation levels were

Table 1. Aggregation levels of peptide-linked (SG3203) versus disulfide-linked (SG3451) ADCs

	Anti-HER2-SG3203 (peptide)		Anti-HER2-SG3451 (disulfide)	
Results	**DAR 2**	**DAR 4**	**DAR 2**	**DAR 4**
Aggregation (before purification)	7.0%	10.7%	2.7%	3.1%
Aggregation (after purification)	4.1%	14.1%	3.3%	4.7%

consistently higher with the peptide-linked ADC anti-HER2-SG3203, with post-purification levels of the DAR 4 ADC unacceptably high for *in vivo* studies (Table 1). Switching to the less hydrophobic disulfide linker (SG3451) afforded an ADC with low levels of aggregation at both DARs as well as before and after purification.

Discussion

Despite the promise ADCs have shown to date as effective therapies for treating human disease, they continue to be limited by their toxicity. A significant amount of effort has been spent on site-specific conjugates, more stable conjugation strategies, and new cytotoxic payloads. There has been less focus on the development of new linkers (32–34) and little published work on the impact of these linkers on efficacy and safety.

Our primary question revolved around the impact of linker type or mechanism of release on the efficacy and toxicity of ADCs. To conceptually address this, we designed and prepared peptide- (SG3203) and disulfide-linked ADCs (SG3231, SG3451) that release the same amine-containing drug. All linkers were connected to a PBD dimer at the nitrogen of one imine, preventing DNA cross-linking until linker cleavage and immolation is complete. The peptide-linked ADC utilizes the same linker as the clinically approved ADCETRIS and a similar linker to the five PBD ADCs in clinical trials, differing by the replacement of alanine with citrulline (8, 35–37). This linker is cleaved by proteases and rapidly releases the free drug in the lysosome.

To setup a stable disulfide to release the PBD, we used a novel disulfide linker utilizing both a new bioconjugation strategy (21) and spacer. These linkers (SG3231, SG3451) rely on the sterics and electronics of the thiol of a cysteine-engineered antibody for stabilization of the disulfide. Taking advantage of the bioreversibility of this stabilization, upon antibody degradation in the lysosome, this stable disulfide linker is made reactive and its putative cysteine catabolite can be reduced in the cytosol by intracellular thiols. Furthermore, incorporation of a short-immolating spacer enables the disulfide ADC to be applied to connect and release amine-containing drugs. Because both disulfide- and peptide-linked ADCs release the exact same PBD drug (SG2057), the difference between these ADCs will be the kinetics and intracellular compartments of free drug release.

Through the use of cysteine engineering we explored the impact of antibody site on disulfide-PBD stability using an ADC with an unhindered disulfide linker (SG3231). This linker-drug was connected to a cysteine-engineered antibody at either V205C of the LC, a site that showed the highest stability for maleimide linker connections (38) or a newly identified site, LC-K149C (21). We discovered that although a PBD linked through a disulfide to site V205C was unstable, site LC-K149C was uniquely able to stabilize the same unhindered disulfide-linked PBD. The efficacy outcome paralleled that of *in vivo* stability, with K149C disulfide-linked ADCs being more efficacious in HER2 models than those linked at V205C.

Further modification with the addition of a single methyl group to the disulfide linker (SG3451) provided an ADC with an even higher level of stability *in vivo* and superior efficacy at the K149C site. This additional methyl group not only improved stability but also increased the rate of free drug release, likely due to an increased rate of cyclization (39).

Having identified a site (LC-K149C) and linker substitution (SG3451, methyl disulfide) with good stability and release for disulfide-linked PBD ADCs, we wanted to compare efficacy and toxicity against that of a peptide-linked PBD ADC (SG3203) that would release the same metabolite. We selected a lymphoma xenograft model to compare the two ADCs because it is more discriminating to linker differences compared to HER2 models (19, 20). Furthermore, three peptide-linked PBD ADCs are being evaluated in clinical trials for lymphoma. We determined that the peptide- and disulfide-linked PBD ADCs provided similar efficacy in two different lymphoma models. Finally, safety studies in rats demonstrated that the disulfide-linked PBD ADC was better tolerated than the peptide-linked PBD ADC. The MTD of the disulfide-linked ADC was 10 mg/kg (the highest dose tested) whereas the MTD of the peptide-linked ADC was 2.5 mg/kg. The decreased toxicity of the disulfide-linked ADC was manifested in both clinical chemistry and anatomic pathology.

In addition to an improved safety profile, we wanted to evaluate the impact of linker on the biophysical properties of the resulting conjugates. The simplicity of the disulfide linker in SG3451 is exemplified in that it only contains a total of 13 atoms with 6 bonds separating the drug from the antibody, whereas the peptide linker in SG3203 is made up of 82 atoms with 24 bonds between the drug and antibody. Furthermore, comprising these 82 atoms are hydrophobic amino acids and a lipophilic aromatic ring. To characterize the impact of these linker differences on conjugate properties, we selected aggregation as a simple measure of physical stability that has implication towards pharmacokinetics as well as towards potential drug development (40). Aggregation is a particular challenge for ADCs utilizing DNA damaging payloads (8, 41–44). The disulfide-linked ADCs (SG3451) showed decreased levels of aggregation compared to the corresponding peptide-linked ADC (SG3203).

Together our results demonstrate the potential for novel linkers to improve the biophysical properties and increase the therapeutic index of ADCs.

Disclosure of Potential Conflicts of Interest

T.H. Pillow has ownership interest (including patents) in Roche Stock and Options. J. Sadowsky is a scientist at Genentech. J. Chen is a research fellow at WuXi Apptec. No potential conflicts of interest were disclosed by the other authors.

Authors' Contributions

Conception and design: T.H. Pillow, S.-F. Yu, W. Solis, D.D. Leipold, A.V. Kamath, L. Masterson, P.W. Howard, J. Gunzner-Toste, S. Spencer, A.G. Polson, J.A. Flygare, J.R. Junutula

Development of methodology: S.-F. Yu, J. Sadowsky, W. Solis, L. Liu, C. Ng, K. Xu, D. Zhang, L. Masterson, S.J. Gregson, P.W. Howard, F. Fang, J. Chen, J.A. Flygare, J.R. Junutula
Acquisition of data (provided animals, acquired and managed patients, provided facilities, etc.): M. Schutten, R. Ohri, J. Sadowsky, W. Solis, G.D. Rosario, M.A.T. Go, J. Lau, S. Yee, J. He, C. Ng, K. Xu, D.D. Leipold, A.V. Kamath, S.J. Gregson, P.W. Howard, F. Fang, J. Chen, J.A. Flygare, J.R. Junutula
Analysis and interpretation of data (e.g., statistical analysis, biostatistics, computational analysis): M. Schutten, S.-F. Yu, R. Ohri, J. Sadowsky, W. Solis, F. Zhong, J. Lau, S. Yee, J. He, C. Ng, K. Xu, D.D. Leipold, A.V. Kamath, L. Masterson, S.J. Gregson, P.W. Howard, S. Spencer, A.G. Polson, J.A. Flygare, J.R. Junutula
Writing, review, and/or revision of the manuscript: T.H. Pillow, M. Schutten, S.-F. Yu, W. Solis, F. Zhong, K. Xu, D.D. Leipold, A.V. Kamath, L. Masterson, S.J. Gregson, P.W. Howard, K.K. Kozak, P. Polakis, J.A. Flygare, J.R. Junutula
Administrative, technical, or material support (i.e., reporting or organizing data, constructing databases): M. Schutten, S.-F. Yu, K.A. Poon, C. Ng, L. Masterson, S.J. Gregson, S. Spencer, J.A. Flygare, J.R. Junutula
Study supervision: S.-F. Yu, K.A. Poon, W. Solis, K. Xu, J.A. Flygare, J.R. Junutula
Other (synthetic chemistry): L. Masterson
Other (involved in identifying new conjugation site and supervised generation of *in vitro* assessments leading to *in vivo* data): K.K. Kozak

Acknowledgments

We thank Josefa Chuh and Sunil Bhakta for their efforts in the initial screen leading to the identification of site LC-K149C and Martine Darwish, Laura Murray, Helga Raab, Blisseth Sy, Breanna Vollmar, and Elmer Wu for helping in the preparation and distribution of the materials described in the study.

The costs of publication of this article were defrayed in part by the payment of page charges. This article must therefore be hereby marked *advertisement* in accordance with 18 U.S.C. Section 1734 solely to indicate this fact.

Received September 29, 2016; revised October 19, 2016; accepted January 24, 2017; published OnlineFirst February 21, 2017.

References

1. Polakis P. Antibody drug conjugates for cancer therapy. Pharmacol Rev 2016;68:3–19.
2. Chari RV. Expanding the reach of antibody–drug conjugates. ACS Med Chem Lett 2016;7:974–76.
3. Liu R, Wang RE, Wang F. Antibody-drug conjugates for non-oncological indications. Expert Opin Biol Ther 2016;16:591–3.
4. Widdison WC, Wilhelm SD, Cavanagh EE, Whiteman KR, Leece BA, Kovtun Y, et al. Semisynthetic maytansine analogues for the targeted treatment of cancer. J Med Chem 2006;49:4392–408.
5. Doronina SO, Toki BE, Torgov MY, Mendelsohn BA, Cerveny CG, Chace DF, et al. Development of potent monoclonal antibody auristatin conjugates for cancer therapy. Nat Biotechnol 2003;21:778–84.
6. Dokter W, Ubink R, van der Lee M, van der Vleuten M, van Achterberg T, Jacobs D, et al. Preclinical profile of the HER2-targeting ADC SYD983/SYD985: introduction of a new duocarmycin-based linker-drug platform. Mol Cancer Ther 2014;13:2618–29.
7. Ricart AD. Antibody-drug conjugates of calicheamicin derivative: gemtuzumab ozogamicin and inotuzumab ozogamicin. Clin Cancer Res 2011;17:6417–27.
8. Jeffrey SC, Burke PJ, Lyon RP, Meyer DW, Sussman D, Anderson M, et al. A potent anti-CD70 antibody-drug conjugate combining a dimeric pyrrolobenzodiazepine drug with site-specific conjugation technology. Bioconjugate Chem 2013;24:1256–63.
9. Miller ML, Fishkin NE, Li W, Whiteman KR, Kovtun Y, Reid EE, et al. A new class of antibody-drug conjugates with potent DNA alkylating activity. Mol Cancer Ther 2016;15:1870–8.
10. Flygare JA, H PT, Aristoff P. Antibody-drug conjugates for the treatment of cancer. Chem Biol Drug Des 2013;81:113–21.
11. Agarwal P, Bertozzi CR. Site-specific antibody-drug conjugates: the nexus of bioorthogonal chemistry, protein engineering, and drug development. Bioconjugate Chem 2015;26:176–92.
12. Chudasama V, Maruani A, Caddick S. Recent advances in the construction of antibody-drug conjugates. Nat Chem 2016;8:114–9.
13. Akkapeddi P, Azizi SA, Freedy AM, Cal P. Construction of homogeneous antibody–drug conjugates using site-selective protein chemistry. Chem Sci 2016;7:2954–63.
14. Nolting B. Linker technologies for antibody-drug conjugates. Methods Mol Biol 2013;1045:71–100.
15. McCombs JR, Owen SC. Antibody drug conjugates: design and selection of linker, payload and conjugation chemistry. AAPS J 2015;17:339–51.
16. Lu J, Jiang F, Lu A, Zhang G. Linkers having a crucial role in antibody-drug conjugates. Int J Mol Sci 2016;17:561.
17. Jain N, Smith SW, Ghone S, Tomczuk B. Current ADC linker chemistry. Pharm Res 2015;32:3526–40.
18. Burke PJ, Senter PD, Meyer DW, Miyamoto JB, Anderson M, Toki BE, et al. Design, synthesis, and biological evaluation of antibody-drug conjugates comprised of potent camptothecin analogues. Bioconjugate Chem 2009;20:1242–50.
19. Lewis Phillips GD, Li G, Dugger DL, Crocker LM, Parsons KL, Mai E, et al. Targeting HER2-positive breast cancer with trastuzumab-DM1, an antibody-cytotoxic drug conjugate. Cancer Res 2008;68:9280–90.
20. Polson AG, Calemine-Fenaux J, Chan P, Chang W, Christensen E, Clark S, et al. Antibody-drug conjugates for the treatment of non-Hodgkin's lymphoma: target and linker-drug selection. Cancer Res 2009;69:2358–64.
21. Pillow TH, Sadowsky JD, Zhang D, Yu S-F, Del Rosario G, Xu K, et al. Decoupling stability and release in disulfide bonds with antibody-small molecule conjugates. Chem Sci 2017;8:366–370.
22. Kim MT, Chen Y, Marhoul J, Jacobson F. Statistical modeling of the drug load distribution on trastuzumab emtansine (kadcyla), a lysine-linked antibody drug conjugate. Bioconjugate Chem 2014;25:1223–32.
23. Junutula JR, Flagella KM, Graham RA, Parsons KL, Ha E, Raab H, et al. Engineered thio-trastuzumab-DM1 conjugate with an improved therapeutic index to target human epidermal growth factor receptor 2-positive breast cancer. Clin Cancer Res 2010;16:4769–78.
24. Gerratana B. Biosynthesis, synthesis, and biological activities of pyrrolobenzodiazepines. Med Res Rev 2012;32:254–93.
25. Xu K, Liu L, Saad OM, Baudys J, Williams L, Leipold D, et al. Characterization of intact antibody-drug conjugates from plasma/serum in vivo by affinity capture capillary liquid chromatography-mass spectrometry. Anal Biochem 2011;412:56–66.
26. Gregson SJ, Howard PW, Gullick DR, Hamaguchi A, Corcoran KE, Brooks NA, et al. Linker length modulates DNA cross-linking reactivity and cytotoxic potency of C8/C8' ether-linked C2-exo-unsaturated pyrrolo[2,1-c][1,4]benzodiazepine (PBD) dimers. J Med Chem 2004;47:1161–74.
27. Hartley JA, Hamaguchi A, Suggitt M, Gregson SJ, Thurston DE, Howard PW. DNA interstrand cross-linking and in vivo antitumor activity of the extended pyrrolo[2,1-c][1,4]benzodiazepine dimer SG2057. Invest New Drugs 2011;30:950–8.
28. Zhang D, Pillow TH, Ma Y, Cruz-Chuh JD, Kozak KR, Sadowsky JD, et al. Linker immolation determines cell killing activity of disulfide-linked pyrrolobenzodiazepine antibody-drug conjugates. ACS Med Chem Lett 2016;7:988–93.
29. Zhang D, Yu S-F, Ma Y, Xu K, Dragovich PS, Pillow TH, et al. Chemical structure and concentration of intratumor catabolites determine efficacy of antibody drug conjugates. Drug Metab Dispos 2016;44:1517–23.
30. Satyam A. Design and synthesis of releasable folate–drug conjugates using a novel heterobifunctional disulfide-containing linker. Bioorg Med Chem Lett 2008;18:3196–9.
31. Li D, Poon KA, Yu S-F, Dere R, Go M, Lau J, et al. DCDT2980S, an anti-CD22-monomethyl auristatin E antibody-drug conjugate, is a potential treatment for non-Hodgkin lymphoma. Mol Cancer Ther 2013;12:1255–65.

32. Staben LR, Koenig SG, Lehar SM, Vandlen R, Zhang D, Chuh J, et al. Targeted drug delivery through the traceless release of tertiary and heteroaryl amines from antibody-drug conjugates. Nature Chem 2016;8:1112–9.
33. Kern JC, Cancilla M, Dooney D, Kwasnjuk K, Zhang R, Beaumont M, et al. Discovery of pyrophosphate diesters as tunable, soluble, and bioorthogonal linkers for site-specific antibody-drug conjugates. J Am Chem Soc 2016;138:1430–45.
34. Kolakowski RV, Haelsig KT, Emmerton KK, Leiske CI, Miyamoto JB, Cochran JH, et al. The methylene alkoxy carbamate self-immolative unit: utilization for the targeted delivery of alcohol-containing payloads with antibody-drug conjugates. Angew Chem Int Ed 2016;55:7948–51.
35. Kung Sutherland MS, Walter RB, Jeffrey SC, Burke PJ, Yu C, Kostner H, et al. SGN-CD33A: a novel CD33-targeting antibody-drug conjugate using a pyrrolobenzodiazepine dimer is active in models of drug-resistant AML. Blood 2013;122:1455–63.
36. Saunders LR, Bankovich AJ, Anderson WC, Aujay MA, Bheddah S, Black K, et al. A DLL3-targeted antibody-drug conjugate eradicates high-grade pulmonary neuroendocrine tumor-initiating cells in vivo. Sci Transl Med 2015;7:302ra136.
37. Flynn M, Zammarchi F, Tyrer PC, Akarca AU, Janghra N, Britten CE, et al. ADCT-301, a pyrrolobenzodiazepine (PBD) dimer-containing antibody drug conjugate (ADC) targeting CD25-expressing hematological malignancies. Mol Cancer Ther 2016;15:2709–21.
38. Shen B-Q, Xu K, Liu L, Raab H, Bhakta S, Kenrick M, et al. Conjugation site modulates the in vivo stability and therapeutic activity of antibody-drug conjugates. Nat Biotechnol 2012;30:184–9.
39. Beesley RM, Ingold CK, Thorpe JF. CXIX—the formation and stability of spiro-compounds. Part I. spiro-compounds from cyclohexane. J Chem Soc Trans 1915;107:1080–106.
40. Chennamsetty N, Voynov V, Kayser V, Helk B, Trout BL. Design of therapeutic proteins with enhanced stability. Proc Natl Acad Sci U S A 2009;106:11937–42.
41. Jeffrey SC, Torgov MY, Andreyka JB, Boddington L, Cerveny CG, Denny WA, et al. Design, synthesis, and in vitro evaluation of dipeptide-based antibody minor groove binder conjugates. J Med Chem 2005;48:1344–58.
42. Jeffrey SC, Nguyen MT, Moser RF, Meyer DL, Miyamoto JB, Senter PD. Minor groove binder antibody conjugates employing a water soluble beta-glucuronide linker. Bioorg Med Chem Lett 2007;17:2278–80.
43. Hollander I, Kunz A, Hamann PR. Selection of reaction additives used in the preparation of monomeric antibody-calicheamicin conjugates. Bioconjugate Chem 2008;19:358–61.
44. Zhao RY, Erickson HK, Leece BA, Reid EE, Goldmacher VS, Lambert JM, et al. Synthesis and biological evaluation of antibody conjugates of phosphate prodrugs of cytotoxic DNA alkylators for the targeted treatment of cancer. J Med Chem 2012;55:766–82.